



1 **Seasonal changes in the D/H ratio of fatty acids of pelagic**
2 **microorganisms in the coastal North Sea**

3 Sandra Mariam Heinzelmann^{#1}, Nicole Jane Bale¹, Laura Villanueva¹, Danielle Sinke-Schoen¹,
4 Catharina Johanna Maria Philippart^{2,3}, Jaap Smede Sinninghe Damsté^{1,4}, Stefan Schouten^{1,4},
5 Marcel Theunis Jan van der Meer¹

6 [1] NIOZ Royal Netherlands Institute for Sea Research, Department of Marine Organic
7 Biogeochemistry, P.O. Box 59, 1790 AB Den Burg, The Netherlands

8 [2] NIOZ Royal Netherlands Institute for Sea Research, Department of Marine Ecology, P.O.
9 Box 59, 1790 AB Den Burg, The Netherlands

10 [3] Utrecht University, Faculty of Geosciences, Department of Physical Geography, Coastal
11 Processes, P.O. box 80.115, 3508 TC Utrecht, The Netherlands

12 [4] Utrecht University, Faculty of Geosciences, Department of Earth Sciences, Geochemistry,
13 P.O. Box 80.021, 3508 TA Utrecht, The Netherlands

14 [#]corresponding author: sandra.heinzelmann@nioz.nl

15 **To be submitted to Biogeosciences**

16

17 Running title: Shift in D/H ratio of fatty acids during seasonal changes in pelagic microbial
18 communities

19 Keywords: metabolism, fatty acids, photoautotrophs, heterotrophs, algal bloom, 16S rRNA
20 gene amplicon pyrosequencing, bacterial diversity, coastal environment, hydrogen isotopes

21



22 **Abstract**

23 Culture studies of microorganisms have shown that the hydrogen isotopic composition of fatty
24 acids depends on their metabolism, but there are only few environmental studies available to
25 confirm this observation. Here we studied the seasonal variability of the deuterium/hydrogen
26 (D/H) ratio of fatty acids in the coastal Dutch North Sea and compared this with the diversity
27 of the phyto- and bacterioplankton. Over the year, the stable hydrogen isotopic fractionation
28 factor ϵ between fatty acids and water ranged between -172‰ and -237‰ , the algal-derived
29 polyunsaturated fatty acid $n\text{C}20:5$ being the most D-depleted and $n\text{C}18:0$ the least D-depleted
30 fatty acid. The D-depleted $n\text{C}20:5$ is in agreement with culture studies, which indicates that
31 photoautotrophic microorganisms produce fatty acids which are significantly depleted in D
32 relative to water. The $\epsilon_{\text{lipid/water}}$ of all fatty acids showed a transient shift towards increased
33 fractionation during the spring phytoplankton bloom, indicated by increasing chlorophyll *a*
34 concentrations and relative abundance of the $n\text{C}20:5$ PUFA, suggesting increased contributions
35 of photoautotrophy. Time periods with decreased fractionation (less negative $\epsilon_{\text{lipid/water}}$ values)
36 can be explained by an increased contribution by heterotrophy to the fatty acid pool. Our results
37 show that the hydrogen isotopic composition of fatty acids is a useful tool to assess the
38 community metabolism of coastal plankton.

39 **1. Introduction**

40 The hydrogen isotopic composition of fatty acids of microorganisms has been shown to depend
41 on different factors like metabolism, salinity, biosynthetic pathways, growth phase and
42 temperature (Dirghangi and Pagani, 2013; Fang et al., 2014; Heinzemann et al., 2015a;
43 Heinzemann et al., 2015b; Zhang et al., 2009a; Zhang et al., 2009b). While most of these factors
44 lead to relatively small variations in the deuterium to hydrogen (D/H) ratio of fatty acids (10-
45 20 ‰), differences in the central metabolism of microorganisms have a much more pronounced
46 effect. Both photo- and chemoautotrophs produce fatty acids depleted in D compared to growth



47 water with the stable hydrogen isotopic fractionation factor ϵ between fatty acids and water
48 ($\epsilon_{\text{lipid/water}}$) ranging between -150 ‰ to -250 ‰ and -250 ‰ and -400 ‰, respectively (Campbell
49 et al., 2009; Chikaraishi et al., 2004; Heinzlmann et al., 2015a; Heinzlmann et al., 2015b;
50 Sessions et al., 2002; Valentine et al., 2004; Zhang et al., 2009a; Zhang and Sachs, 2007). In
51 contrast, heterotrophs produce fatty acids with either a relatively minor depletion or an
52 enrichment in D compared to the growth water with $\epsilon_{\text{lipid/water}}$ values ranging between -150 ‰
53 and +200 ‰ (Dirghangi and Pagani, 2013; Fang et al., 2014; Heinzlmann et al., 2015a;
54 Heinzlmann et al., 2015b; Sessions et al., 2002; Zhang et al., 2009a). The differences in
55 hydrogen isotopic composition of fatty acids produced by organisms expressing different core
56 metabolisms have mainly been attributed to the D/H ratio of nicotinamide adenine dinucleotide
57 phosphate (NADPH) (Zhang et al., 2009a). NADPH can be generated by a variety of different
58 reactions in different metabolic pathways (each associated with different hydrogen isotopic
59 fractionations) and is subsequently used as the main source of hydrogen in lipid biosynthesis
60 (Robins et al., 2003; Saito et al., 1980; Schmidt et al., 2003).

61 Although the metabolism of a microorganism in pure culture is reflected by the D/H ratio of its
62 fatty acids, it is not clear if the D/H ratio of fatty acids from environmental microbial
63 communities can be used to assess the ‘integrated’ core metabolisms in nature. Culture
64 conditions rarely represent environmental conditions since cultures are typically axenic and use
65 a single substrate, they do not take into account microbial interactions, and they test a limited
66 number of potential substrates, energy sources and core metabolisms. Previous studies observed
67 a wide range in the D/H ratio of lipids in both water column and sediment (Jones et al., 2008;
68 Li et al., 2009), suggesting inputs of organisms with a variety of metabolisms. So far, one
69 environmental study has been performed that links the D/H ratio of fatty acids from naturally
70 occurring microbial communities to metabolisms possibly expressed by the members of those
71 communities (Osburn et al., 2011). This study showed that different microbial communities



72 from various hot springs in Yellowstone National Park produce fatty acids with hydrogen
73 isotopic compositions in line with the metabolism expressed by the source organism. The D/H
74 ratio of specific fatty acids, which could be attributed to microorganisms expressing a specific
75 core metabolism, was within the range expected for that metabolism. On the other hand, the
76 D/H ratio of common or general fatty acids (e.g. *n*C16:0) allowed for assessing the metabolism
77 of the main contributors of these more general fatty acid, but not necessarily the metabolism of
78 the dominant community members (Osburn et al., 2011). These results show the applicability
79 of this new method, but the ecosystems in which it was tested (hot spring microbial
80 communities) are considered to be of relatively low diversity. Therefore, this method needs to
81 be applied and evaluated in more complex and diverse microbial communities.

82 Here, we studied the seasonal variability of the hydrogen isotopic composition of fatty acids
83 from coastal North Sea water sampled from the jetty at the Royal Netherlands Institute for Sea
84 Research (NIOZ) in order to examine the relationship between hydrogen isotope fractionation
85 in fatty acids and the general metabolism of the community. Time series studies have been
86 previously performed at the NIOZ jetty to determine phytoplankton and prokaryotic abundances
87 and composition (Alderkamp et al., 2006; Brandsma et al., 2012; Brussaard et al., 1996;
88 Philippart et al., 2010; Philippart et al., 2000; Pitcher et al., 2011; Sintes et al., 2013), lipid
89 composition (Brandsma et al., 2012; Pitcher et al., 2011), and chlorophyll *a* concentration
90 (Philippart et al., 2010). Typically, the spring bloom in the coastal North Sea is predominantly
91 formed by *Phaeocystis globosa*, followed directly by a bloom of various diatom species, a
92 second moderate diatom bloom of *Thalassiosira spp.* and *Chaetoceros socialis* that occurs in
93 early summer and an autumn bloom is formed by *Thalassiosira spp.*, *C. socialis*, cryptophytes
94 and cyanobacteria (Brandsma et al., 2012; Cadée and Hegeman, 2002), although the autumn
95 bloom seems to have weakened over the last years (Philippart et al., 2010). The abundance of
96 bacteria co-varies with algal blooms and the bacteria are dominated by heterotrophs, e.g.



97 bacteria belonging to the *Bacteroidetes* (Alderkamp et al., 2006), using released organic matter
98 from declining phytoplankton blooms as carbon, nitrogen and phosphate sources. The intact
99 polar lipid (IPL) composition of the microbial community was shown to be composed mainly
100 of phospholipids, sulfoquinovosyldiacylglycerol and betaine lipids with a limited taxonomic
101 potential (Brandsma et al., 2012). The main source of those lipids was assumed to be the
102 eukaryotic plankton.

103 This well studied site should allow us to trace the shift from an environment dominated by
104 photoautotrophs during major phytoplankton blooms, towards an environment with a higher
105 abundance of heterotrophic bacteria following the end of the bloom. These shifts in the
106 community structure should be reflected in the D/H ratio of fatty acids. We, therefore, analysed
107 the D/H ratio of polar lipid derived fatty acids (PLFA) over a seasonal cycle and compared this
108 with phytoplankton composition data and abundance and information on the bacterial diversity
109 obtained by 16S rRNA gene amplicon sequencing.

110 **2. Material and Methods**

111 **2.1. Study site and sampling**

112 Surface water samples were collected from September 2010 until December 2011 from the
113 NIOZ sampling jetty in the Marsdiep at the western entrance of the North Sea into the Wadden
114 Sea at the island of Texel (53°00'06" N 4°47'21" E). Samples were taken during high tide to
115 ensure that the water sampled was North Sea water.

116 For lipid analysis measured volumes of water (ca. 9-11 L) were filtered consecutively, without
117 pre filtration, through pre-ashed 3 and 0.7 µm pore size glass fibre filters (GF/F, Whatman; 142
118 mm diameter) and stored at -20 °C until lipid extraction. For DNA analysis approximately 1 L



119 seawater was filtered through a polycarbonate filter (0.2 μm pore size; 142 mm diameter;
120 Millipore filters) and stored at $-80\text{ }^{\circ}\text{C}$ until extraction.

121 Salinity measurements were done during the time of sampling with either an Aanderaa
122 Conductivity/Temperature sensor 3211 connected to an Aanderaa datalogger DL3634
123 (Aanderaa Data Instruments AS, Norway) or a Refractometer/Salinometer Endeco type 102
124 handheld (Endeco, USA).

125 For chlorophyll *a* measurements 500 mL sea water was filtered through a 47 mm GF/F filter
126 (0.7 μm pore size, Whatman, GE Healthcare Life Sciences, Little Chalfont, UK) and
127 immediately frozen in liquid nitrogen. Samples were thawed and homogenised with glass beads
128 and extracted with methanol. Chlorophyll *a* concentration was measured with a Dionex high-
129 performance liquid chromatography (HPLC) (Philippart et al., 2010).

130 Water samples for salinity versus $\delta\text{D}_{\text{water}}$ calibration (see below) were sampled weekly between
131 March and September 2013 at high tide. Salinity was determined using a conductivity meter
132 (VWR EC300) calibrated to IAPSO standard seawater of salinities 10, 30, 35 and 37.

133 **2.2. Polar lipid derived fatty acids**

134 Filters were extracted for IPLs and eventually fatty acid analysis. The 0.7 μm filters did not
135 yield enough total lipid extract for analysis. Therefore, only fatty acids obtained from the 3 μm
136 filters were analysed. Due to fast clogging of the filters and a corresponding decrease of the
137 pore size (Sørensen et al., 2013), the 3 μm filters will most likely contain most of the
138 microorganisms present in North Sea water. Freeze dried filters were extracted via a modified
139 Bligh-Dyer method (Bligh and Dyer, 1959; Rütters et al., 2002) with methanol
140 (MeOH)/dichloromethane (DCM)/phosphate buffer (2:1:0.8, vol/vol/vol) using ultrasonication
141 (Heinzelmann et al., 2014). Approximately 0.5 - 1 mg of the Bligh-Dyer extract (BDE) was
142 separated into a neutral and polar lipid fraction using silica column chromatography



143 (Heinzelmann et al., 2014). The BDE was added onto a DCM pre-rinsed silica column (0.5 g;
144 activated for 3 h at 150°C) and eluted with 7 mL of DCM and 15 mL of MeOH. The resulting
145 fractions were dried under nitrogen and stored at -20 °C. PLFAs were obtained via
146 saponification of the MeOH fraction with 1 N KOH in MeOH (96%). The samples were
147 refluxed at 140 °C for 1 h. Afterwards the pH was adjusted to 5 with 2 N HCl/MeOH (1/1),
148 bidistilled H₂O and DCM were added. The MeOH/H₂O layer was washed twice with DCM, the
149 DCM layers were combined and dried over Na₂SO₄. The sample was dried under nitrogen and
150 stored in the fridge. The PLFAs were methylated with boron trifluoride-methanol (BF₃-MeOH)
151 for 5 min at 60 °C. Afterwards H₂O and DCM were added. The H₂O/MeOH layer was washed
152 three times with DCM, and potential traces of water were removed over a small Na₂SO₄ column
153 after which the DCM was evaporated under a stream of nitrogen. In order to obtain a clean
154 PLFA fraction for isotope analysis, the methylated extract was separated over an aluminium
155 oxide (Al₂O₃) column, eluting the methylated PLFAs with three column volumes of DCM. For
156 identification of the position of double bonds in unsaturated fatty acids, the methylated PLFAs
157 were derivatised with dimethyldisulfide (DMDS) (Nichols et al., 1986). Hexane, DMDS and
158 I₂/ether (60 mg/mL) were added to the fatty acids and incubated at 40 °C overnight. After adding
159 hexane, the iodine was deactivated by addition of a 5% aqueous solution of Na₂S₂O₃. The
160 aqueous phase was washed twice with hexane. The combined hexane layers were cleaned over
161 Na₂SO₄ and dried under a stream of nitrogen. The dried extracts were stored at 4 °C.

162 **2.3. Fatty acid and hydrogen isotope analysis**

163 The fatty acid fractions were analysed by gas chromatography (GC) using an Agilent 6890 gas
164 chromatograph with a flame ionization detector (FID) using a fused silica capillary column (25
165 m x 320 µm) coated with CP Sil-5 (film thickness 0.12 µm) with helium as carrier gas. The
166 temperature program was as follows: initial temperature 70 °C, increase of temperature to 130
167 °C with 20 °C min⁻¹, and then to 320 °C with 4 °C min⁻¹ which was kept for 10 min. Individual



168 compounds were identified using GC/mass spectrometry (GC/MS) and the position of the
169 double bonds in unsaturated fatty acids was determined after derivatisation with
170 dimethyldisulfide (Heinzelmann et al., 2015b).

171 Hydrogen isotope analysis of the fatty acid fraction was performed by GC thermal conversion
172 isotope ratio monitoring MS (GC/TC/irMS) using an Agilent 7890 GC connected via Thermo
173 GC Isolink and Conflo IV interfaces to a Thermo Delta V MS according to Chivall et al. (2014).
174 Samples were injected onto an Agilent CP-Sil 5 CB column (25 m × 0.32 mm ID; 0.4 μm film
175 thickness; He carrier gas, 1.0 mL min⁻¹). The GC temperature program was 70 °C to 145 °C at
176 20 °C min⁻¹, then to 320 °C at 4 °C min⁻¹ where it was kept for 15 min. Eluting compounds
177 were converted to H₂ at 1420°C in an Al₂O₃ tube before introduction into the mass spectrometer.
178 The H³⁺ correction factor was determined daily and was constant at 5.3±0.2. A set of standard
179 *n*-alkanes with known isotopic composition (Mixture B prepared by Arndt Schimmelmann,
180 University of Indiana) was analyzed daily prior to analyzing samples in order to monitor the
181 system performance. Samples were only analyzed when the *n*-alkanes in Mix B had an average
182 deviation from their off-line determined value of <5 ‰. An internal standard, squalane (δD = -
183 170 ‰) was co-injected with each fatty acid sample fraction in order to monitor the precision
184 of the measurements over time with δD = -164±4 ‰. The δD of the individual fatty acids was
185 measured in duplicates and corrected for the added methyl group (Heinzelmann et al., 2015b).
186 δD of water samples was determined by elemental analysis/TC/irMS (EA/TC/irMS) according
187 to Chivall et al. (2014).

188 **2.4. Phytoplankton abundance and diversity**

189 Phytoplankton samples were preserved with acid Lugol's iodine, and cells were counted with a
190 Zeiss inverted microscope using 3 mL counting chambers. Most algae were identified to species
191 level, but some were clustered into taxonomic and size groups (Philippart et al., 2000). For each



192 sampling date in the period from September 2010 to December 2011, the densities of the most
193 abundant phytoplankton species or species' groups were calculated. The three most dominant
194 algal species (or groups) together comprised, on average, more than 60% of the total numbers
195 of marine algae in the Marsdiep during this study period.

196 **2.5. DNA extraction**

197 The 0.2 µm polycarbonate filters were defrosted and cut into small pieces with sterile scissors
198 and then transferred into a 50 mL falcon tube. Filter pieces were lysed by bead-beating with ~1
199 g of sterile 0.1 mm zirconium beads (Biospec, Bartlesville, OK) in 10 mL RLT buffer (Qiagen)
200 and 100 µL β-mercaptoethanol for 10 min. 1/60 volume RNase A (5 µg/µL) was added to the
201 lysate, incubated for 30 min at 37 °C and afterwards cooled down for 5 min on ice. The lysate
202 was purified with the DNeasy Blood and Tissue kit (Qiagen, Hilden). DNA was eluted with 3x
203 100 µL AE buffer, the eluates pooled and reconcentrated. DNA quality and concentration was
204 estimated by Nanodrop (Thermo Scientific, Waltham, MA) quantification.

205 **2.6. 16S rRNA gene amplicon sequencing and analysis**

206 The general bacterial diversity was assessed by 16S rRNA gene amplicon pyrotag sequencing.
207 The extracted DNA was quantified fluorometrically with Quant-iT™ PicoGreen® dsDNA
208 Assay Kit (Life Technologies, The Netherlands).

209 PCR reactions were performed with the universal (Bacteria and Archaea) primers S-D-Arch
210 0519-a-S-15 (5'-CAG CMG CCG CGG TAA-3') and S-D-Bact-785-a-A-21 (5'-GAC TAC
211 HVG GGT ATC TAA TCC-3') (Klindworth et al., 2012) adapted for pyrosequencing by the
212 addition of sequencing adapters and multiplex identifier (MID) sequences. To minimize bias
213 three independent PCR reactions were performed containing: 16.3 µL H₂O, 6 µL HF Phusion
214 buffer, 2.4 µL dNTP (25 mM), 1.5 µL forward and reverse primer (10 µM; each containing an



215 unique MID tail), 0.5 μ L Phusion Taq and 2 μ L DNA (6 ng/ μ L). The PCR conditions were
216 following: 98 °C, 30 s; 25 \times [98 °C, 10 s; 53 °C, 20 s; 72 °C, 30 s]; 72 °C, 7 min and 4 °C, 5 min.

217 The PCR products were loaded on a 1% agarose gel and stained with SYBR® Safe (Life
218 Technologies, The Netherlands). Bands were excised with a sterile scalpel and purified with
219 Qiaquick Gel Extraction Kit (QIAGEN, Valencia, CA) following the manufacturer's
220 instructions. PCR purified products were quantified with Quant-iT™ PicoGreen® dsDNA
221 Assay Kit (Life Technologies, The Netherlands). Equimolar concentrations of the barcoded
222 PCR products were pooled and sequenced on GS FLX Titanium platform (454 Life Sciences)
223 by Macrogen Inc. Korea.

224 Samples were analyzed using the QIIME pipeline (Caporaso et al., 2010). Raw sequences were
225 demultiplexed and then quality-filtered with a minimum quality score of 25, length between
226 250–350 bp, and allowing maximum two errors in the barcode sequence. Sequences were then
227 clustered into operational taxonomic units (OTUs, 97% similarity) with UCLUST (Edgar,
228 2010). Reads were aligned to the Greengenes Core reference alignment (DeSantis et al., 2006)
229 using the PyNAST_algorithm (Caporaso et al., 2010). Taxonomy was assigned based on the
230 Greengenes taxonomy and a Greengenes reference database (version 12_10) (McDonald et al.,
231 2012; Werner et al., 2012). Representative OTU sequences assigned to the specific taxonomic
232 groups were extracted through classify.seqs and get.lineage in Mothur (Schloss et al., 2009) by
233 using the Greengenes reference and taxonomy files. The 16S rRNA gene amplicon reads (raw
234 data) have been deposited in the NCBI Sequence Read Archive (SRA) under BioProject number
235 PRJNA293285.

236 **2.7. Phylogenetic analyses**

237 The phylogenetic affiliation of the 16S rRNA gene sequences was compared to release 119 of
238 the Silva NR SSU Ref database (<http://www.arb-silva.de/>; Quast (2012)) using the ARB



239 software package (Ludwig et al., 2004). Sequences were added to the reference tree supplied
240 by the Silva database using the ARB Parsimony tool.

241 **3. Results**

242 Suspended particulate matter (SPM) of North Sea coastal water was obtained during a period
243 from August 2010 - December 2011, covering a complete annual cycle, in approximately
244 biweekly resolution.

245 **3.1. Chlorophyll *a* concentration and phytoplankton abundance and diversity**

246 Chlorophyll *a* concentrations ranged between 0.4 and 22.2 $\mu\text{g L}^{-1}$ (Fig. 1; Table S1). During
247 late autumn, winter and early spring concentrations were low at $\sim 4 \mu\text{g L}^{-1}$. A peak in the
248 chlorophyll *a* concentration occurred in the beginning of April and values stayed relatively high
249 during this month, indicative of the spring bloom. Subsequently, the chlorophyll *a* concentration
250 decreased again, reaching pre-bloom levels and stayed relatively constant thereafter.

251 Phytoplankton diversity and abundance was determined using light microscopy and the two to
252 three most abundant phytoplankton species were identified and counted (Table S2). The
253 majority of the phytoplankton was composed of *Phaeocystis globosa*, diatoms and
254 cyanobacteria (Fig. 2), with the spring bloom primarily being made up of *P. globosa*. The
255 highest abundance of diatoms was also during spring, while the cyanobacteria reached the
256 highest abundance in the beginning of the sampling period from autumn until late winter and
257 again during summer.

258 **3.2. Microbial diversity**

259 To assess bacterial diversity, 16S rRNA gene amplicon sequencing was performed on
260 approximately half of the SPM samples (Table S3).



261 The bacteria detected consisted mainly of members of *Actinobacteria*, *Bacteroidetes*,
262 *Planctomycetes*, α -*Proteobacteria*, β -*Proteobacteria*, γ -*Proteobacteria* and *Verrucomicrobia*
263 (Fig. 3; Table S3). The majority of the reads belonged to the orders of the *Flavobacteriales*,
264 *Rhodobacteriales*, *Rickettsiales*, *Alteromonadales* and *Oceanospirillales*. The *Flavobacteriales*
265 contributed between 12 to 32 % to the total bacterial reads with a relatively constant percentage
266 of ~ 15 % during autumn and winter. The percentage of reads increased during early spring
267 with the highest values from beginning of April until the end of May. The percentage of reads
268 attributed to the *Flavobacteriales* decreased during summer and early autumn. Sequence reads
269 affiliated to the *Rhodobacteriales* (6 to 12 %) and *Rickettsiales* (3 to 17 %) were the most
270 represented within the α -*Proteobacteria*. The percentage of *Rhodobacteriales* reads was fairly
271 constant with no obvious seasonal pattern. In contrast, the percentage of *Rickettsiales* reads
272 followed a distinct seasonal pattern with a maximum in April (up to 17 %) and a minimum in
273 June (3 %). *Alteromonadales* reads made up between 9 and 17 % of all bacteria reads and were
274 fairly constant over the season. The percentage of *Oceanospirillales* reads were between 3 and
275 12 % of the total bacteria reads and show a clear maximum during mid-April (Fig. 3; Table S3).

276 For a more accurate taxonomic classification of the bacterial groups, sequence reads of the
277 *Bacteroidetes*, α -*Proteobacteria* and γ -*Proteobacteria* were extracted from the dataset and a
278 phylogenetic tree was constructed (Fig. S1-S3). Within the *Flavobacteriales* (*Bacteroidetes*)
279 the majority of the reads fell either within the *Cryomorphaceae* or the *Flavobacteriaceae* with
280 sequences clustering within *Fluviicola* and *Crocinitomix*, *Flavobacterium* and *Tenacibaculum*,
281 respectively. Within the *Rhodobacteriales* (α -*Proteobacteria*) most of the reads belonged to
282 *Rhodobacteraceae* and sequences within this family were closely related to the genus
283 *Octadecabacter*. Within the *Rickettsiales* most of the reads were affiliated to the
284 *Pelagibacteraceae* (SAR11 cluster). The majority of the γ -*Proteobacteria* reads were classified
285 within the *Alteromonadales* and *Oceanospirillales*. The *Alteromonadales* reads and sequences



286 fell within the uncultured *HTCC2188*-isolate and *OM60*-clade and various members of the
287 *Alteromonadaceae*-family. The *Halomonadaceae* family comprised most of the
288 *Oceanospirillales* reads and additionally sequences clustered with various members of the
289 *Oceanospirillaceae*.

290 3.3. Fatty acid distribution in North Sea SPM

291 Polar lipid derived fatty acids were comprised of *nC14:0*, *nC16:1 ω 7*, *nC16:0*, *nC18:0*, the
292 polyunsaturated fatty acid (PUFA) *nC20:5*, and various unsaturated *nC18* fatty acids (Fig. 4;
293 Table S4). The *nC14:0* fatty acid followed a seasonal cycle with the lowest relative abundance
294 during winter, and the highest from June to August (Fig. 4a). The *nC16:0* fatty acid was the
295 dominant fatty acid (21–38 %) with no clear seasonal pattern (Fig. 4c). The *nC16:1* fatty acid
296 was the next most abundant fatty acid (13–35 %) with a maximum from March to April (Fig.
297 4b). Various unsaturated *nC18:x* fatty acids were observed throughout the season. Due to low
298 abundance of the individual fatty acids and co-elutions the double bond positions could not be
299 determined. These unsaturated fatty acids made up 9–30 % of all fatty acids (Fig. 4d). The
300 *nC18:0* fatty acid had relative abundances varying between 2–18 % with the highest relative
301 abundance during autumn months (10–18 %) and the lowest during spring, 2–6 % (Fig. 4e). A
302 *nC20:5* PUFA (Fig. 4f) was observed in most samples with the highest relative abundance
303 during March and April (11–14 %) and early August (18 %). Trace amounts of *nC15:0*, *iC15:0*
304 and *aiC15:0* fatty acids were also detected.

305 3.4. Hydrogen isotopic composition of fatty acids

306 δ D values of *nC14:0*, *nC16:1 ω 7*, *nC16:0*, *nC18:0* fatty acids and *nC20:5* were obtained for most
307 of the samples (Table S5). The D/H ratio of the other fatty acids could not be determined with
308 sufficient accuracy due to either incomplete separation or low abundance.



309 In general, *n*C14:0 and *n*C20:5 were the most depleted fatty acids with δD values ranging
310 between -198 to -241 ‰ and -180 to -241 ‰, respectively. The *n*C18:0 was typically the fatty
311 acid with the highest δD values ranging between -175 to -212 ‰ (Table S5).

312 4. Discussion

313 4.1. Hydrogen isotopic fractionation expressed in fatty acids

314 For the proper assessment of the impact of metabolism on the hydrogen isotopic composition
315 of fatty acids the hydrogen isotopic fractionation of the fatty acids versus water is required
316 ($\epsilon_{\text{lipid/water}}$). For this, the δD of the water (δD_{water}) at the time of sampling is needed. However,
317 at the time of sampling of the SPM unfortunately no water samples were taken and preserved
318 for δD analysis. Therefore, we used an alternative approach to estimate δD_{water} using the salinity
319 of the water measured at the time of sampling. A strong correlation between salinity and δD_{water}
320 is generally observed in marine environments since both parameters depend on evaporation,
321 precipitation and freshwater influx (Craig and Gordon, 1965; Mook, 2001). To establish a local
322 salinity - δD_{water} correlation, water samples were collected weekly during high tide (March to
323 September 2013) and salinity and δD_{water} were measured. Indeed, a strong correlation between
324 salinity and δD_{water} is observed ($R^2=0.68$; Fig. S4). Using this correlation and the salinities
325 measured, we reconstructed δD_{water} values at the time of sampling of the biomass (Table 1). The
326 error in the estimate of $\epsilon_{\text{lipid/water}}$ resulting from this approach is approximately 1.5 ‰, which is
327 less than the error in the determination of δD of the fatty acids (1-12 ‰).

328 All fatty acids were depleted in D compared to water with the fractionation factor $\epsilon_{\text{lipid/water}}$
329 ranging from -173 to -237 ‰, all following a similar seasonal trend with the highest degree of
330 fractionation during spring to early summer, and early autumn (Fig. 5; Table 1). The lowest



331 degree of fractionation (most positive $\epsilon_{\text{lipid/water}}$ values) was in general during late autumn and
332 the winter months.

333 **4.2. Source affects the hydrogen isotopic composition of individual fatty acids**

334 The *n*C20:5 PUFA is the most specific fatty acid detected in North Sea SPM and is exclusively
335 produced by algae (Carrie et al., 1998). The *n*C20:5 PUFA is one of the most D-depleted fatty
336 acids (Fig. 5), which is in agreement with culture studies that show that photoautotrophic
337 microorganisms produce fatty acids that are depleted in D with $\epsilon_{\text{lipid/water}}$ values between -162
338 and -215 ‰, while heterotrophic microorganisms on the other hand produce fatty acids with
339 $\epsilon_{\text{lipid/water}}$ values ranging between -150 to +200 ‰. Furthermore, its concentration increased at
340 the time of the phytoplankton bloom (Fig. 4). Interestingly, after the phytoplankton bloom,
341 when the abundance of pelagic algae had decreased (Fig. 4), it became more enriched in D (Fig.
342 5). This enrichment might be due to changes in the relative contribution of source organisms.
343 In diatoms *n*C20:5 PUFA can be one of the most abundant fatty acids, while *Phaeocystis*
344 produces it in minor amounts only (Table S6). During the spring bloom both organisms will
345 contribute to the fatty acid pool, while afterwards diatoms are the main source (Fig. 2; Table
346 S2). Another possible reason could be that after the bloom and due to nutrient limitation,
347 phytoplankton might use more storage products leading to an increased production of NADPH
348 via other pathways than photosynthesis. The NADPH produced by photoautotrophs via
349 photosystem I is depleted in D (Zhang et al., 2009a), while NADPH produced via the pentose
350 phosphate (OPP) pathway and the tricarboxylic acid (TCA) cycle is relatively enriched in D
351 (Heinzelmann et al., 2015b; Zhang et al., 2009a). The utilization of storage products would lead
352 to an increased production of NADPH via both the OPP pathway and the TCA cycle leading to
353 more positive $\epsilon_{\text{lipid/water}}$ values of the *n*C20:5 PUFA after the bloom.



354 Of all other fatty acids $nC14:0$ was generally the most D-depleted fatty acid, possibly suggesting
355 a higher contribution of photoautotrophic organisms to this fatty acid. The quite similar $\epsilon_{\text{lipid/water}}$
356 values of $nC16:1$ (-179 to -224 ‰) and $nC16:0$ (-178 to -215 ‰) relatively to each other suggest
357 similar sources for the two fatty acids. The least negative $\epsilon_{\text{lipid/water}}$ values for $nC18:0$ suggest
358 that the sources of this fatty acid might differ from the other fatty acids i.e. with a higher
359 contribution of heterotrophs compared to the other fatty acids.

360 Fatty acids profiles of representatives of most members of the phytoplankton and bacterial
361 community observed at our site have been previously reported (Table S6) and can be used to
362 assess the main sources of the different fatty acid pools. The main bacterial contributors to the
363 $nC16:0$ and $nC16:1\omega7$ fatty acids are most likely members of the *Alteromonadales* and the
364 *Halomonadaceae*, while the majority of bacterial contributors to the $nC14:0$ and $nC18:0$ fatty
365 acid are derived from the *Puniceococcales* (Table S6). Both the *Flavobacteriales* and the
366 *Rhodobacteriaceae*, which make up a large part of the total bacteria reads, will hardly contribute
367 to the measured isotopic signal as they have been reported to produce only traces of $nC14:0$,
368 $nC16:0$, $nC16:1\omega7$ or $nC18:0$ fatty acids (Table S6). The observed phytoplankton species are
369 main contributors to the $nC14:0$, $nC16:0$ and $nC16:1\omega7$ fatty acid pools, but contribute
370 relatively little to the $nC18:0$ fatty acid pools. *Phaeocystis* produces mainly the $nC14:0$ and
371 $nC16:0$ fatty acids (Hamm and Rousseau, 2003; Nichols et al., 1991).

372 Overall, the majority of the $nC14:0$ fatty acid pool will likely be predominately derived from
373 photoautotrophs (Table S6), which potentially explains why the $nC14:0$ is almost always the
374 most depleted fatty acid. The $nC18:0$ fatty acid on the other hand, will be mainly derived from
375 heterotrophic bacteria (Table S6) resulting in more D enriched signal compared to that of the
376 $nC14:0$ fatty acid.



377 Culture studies have shown that chemoautotrophs produce fatty acids, which are even more
378 depleted in D compared to photoautotrophs. However, none of the fatty acids measured in the
379 North Sea SPM have $\epsilon_{\text{lipid/water}}$ values which fall in the range of those predicted for
380 chemoautotrophs (-264 to -345 ‰; Heinzemann et al., 2015b). This fits with the observation
381 that sequence reads of chemoautotrophic bacteria accounted for < 3 % of the total bacterial
382 reads (Fig. 3; Table S3), and thus it is unlikely that this metabolism plays an important role in
383 this environment.

384 **4.3. Linking seasonal changes of hydrogen isotope fractionation to changes in community** 385 **metabolism**

386 All the fatty acids showed a similar seasonal trend with the most negative ϵ values in spring and
387 the most positive ϵ values in the winter (Fig. 5). In order to assess the dominant metabolism of
388 the whole microbial community we calculated a weighted average ϵ of all measured fatty acids
389 apart from the specific *n*C20:5 PUFA. The weighted average $\epsilon_{\text{lipid/water}}$ ($\epsilon_{\Sigma\text{FA}}$) followed the same
390 seasonal trend as the $\epsilon_{\text{lipid/water}}$ values of the individual fatty acids (Fig. 1+5), and ranged between
391 -180 and -225 ‰ with an average of -199 ‰.

392 Compared to the chlorophyll *a* concentration, the $\epsilon_{\Sigma\text{FA}}$ followed an opposite seasonal trend i.e.
393 when the chlorophyll *a* concentration increased in early April, $\epsilon_{\Sigma\text{FA}}$ decreased (Fig. 5). The
394 chlorophyll *a* maximum in April-May indicates a spring bloom (Fig. 2), which is known to
395 occur annually in North Sea coastal waters (Brandsma et al., 2012; Philippart et al., 2010) and
396 corresponds with a shift towards more negative values for $\epsilon_{\Sigma\text{FA}}$, as well as a high abundance of
397 the algal-derived *n*C20:5 PUFA (Fig. 4). It is likely that at least during the spring bloom the
398 majority of the fatty acids are derived from the dominant algae, i.e. *Phaeocystis* and diatoms,
399 which make up the majority of the bloom, leading to a D depleted signal. Thus, the observation
400 that the value of $\epsilon_{\Sigma\text{FA}}$ was more negative during the spring bloom when the environment is



401 dominated by photoautotrophic microorganisms (Fig. 3) fits with an increased contribution by
402 photoautotrophs relative to heterotrophic microorganisms to the fatty acid pool. At the end of
403 the bloom more positive $\epsilon_{\Sigma\text{FA}}$ values were observed, which is in agreement with an increased
404 abundance of heterotrophic bacterioplankton in previous studies (Sintes et al., 2013), living on
405 released organic material (Alderkamp et al., 2006). Interestingly, analysis of suspended
406 particulate matter from the California borderland basins also showed that typical bacterial fatty
407 acids were generally enriched in D while algal fatty acids were more depleted in D (Jones et al.,
408 2008), similar to what we observed here.

409 Thus, $\epsilon_{\Sigma\text{FA}}$ values reflect a mixed signal derived from mainly photoautotrophic and, to a lesser
410 extent, heterotrophic microorganisms. Nevertheless, $\epsilon_{\text{lipid/water}}$ values for all fatty acids remain
411 in the range of photoautotrophic metabolism (Heinzelmann et al., 2015b), indicating that,
412 overall, the fatty acids in this coastal seawater are mostly derived from phototrophic organisms.
413 This is in accordance with the assumption that IPLs (containing fatty acids) in coastal North
414 Sea waters over the annual cycle were predominantly derived from phytoplankton (Brandsma
415 et al., 2012). Our results show that it is possible to study whole community core metabolism in
416 a natural environment by determining the weighted average D/H ratio of all fatty acids.

417 **5. Conclusion**

418 A seasonal study of fatty acids derived from the coastal Dutch North Sea shows that all fatty
419 acids are depleted in D with δD ranging between -174 and -241 ‰. The most negative values
420 were observed during the spring bloom, when the biomass is dominated by photoautotrophic
421 microorganisms. The subsequent higher relative contribution of heterotrophs to the general fatty
422 acid pools leads to shift in $\epsilon_{\text{lipid/water}}$ towards more positive values by up to 20 ‰. This shift
423 towards more positive values is in agreement with observations from culture studies where
424 heterotrophic organisms fractionate much less or even opposite to photoautotrophic organisms.



425 This study confirms that hydrogen isotopic fractionation as observed in general fatty acids can
426 be used to study the core metabolism of complex environments and to track seasonal changes
427 therein.

428 **Data availability**

429 Data is available on Pangea under doi:10.1594/PANGAEA.859031

430 **Author Contribution**

431 N.J. Bale helped by providing samples and helped with sampling; L. Villanueva helped with
432 carrying out sequencing experiments and analysis of subsequent data; D. Sinke-Schoen helped
433 with measuring the hydrogen isotopic composition of North Sea water samples; C. J. M.
434 Philippart provided chlorophyll *a* and phytoplankton data; J. S. Sinninghe Damsté, S. Schouten
435 and M. T. J. van der Meer helped design experiments and contributed to the manuscript as
436 supervisors of S.M. Heinzelmann; S.M. Heinzelmann prepared the manuscript with
437 contributions of all co-authors.

438

439 **Acknowledgment**

440 The authors would like to thank Y. A. Lipsewers, E. Svensson and K. K. Sliwiska for their
441 help with sampling. We would like to thank E. Wagemaakers for providing salinity data, M.
442 Veenstra and A. van den Oever for assistance with the phytoplankton sampling and analyses,
443 and M. Verweij for assistance with the GC-MS measurements. MvdM was funded by the Dutch
444 Organisation for Scientific Research (NWO) through a VIDI grant.



445 **References**

446 Alderkamp, A. C., Sintes, E., and Herndl, G. J.: Abundance and activity of major groups of
447 prokaryotic plankton in the coastal North Sea during spring and summer, *Aquat. Microb. Ecol.*,
448 45, 237-246, 10.3354/ame045237, 2006.

449 Bligh, E. G., and Dyer, W. J.: A rapid method of total lipid extraction and purification, *Can J*
450 *Biochem Physiol*, 37, 911-917, 10.1139/o59-099, 1959.

451 Brandsma, J., Hopmans, E. C., Philippart, C. J. M., Veldhuis, M. J. W., Schouten, S., and
452 Sinninghe Damsté, J. S.: Low temporal variation in the intact polar lipid composition of North
453 Sea coastal marine water reveals limited chemotaxonomic value, *Biogeosciences*, 9, 1073-
454 1084, 10.5194/bg-9-1073-2012, 2012.

455 Brussaard, C. P. D., Gast, G. J., van Duyl, F. C., and Riegman, R.: Impact of phytoplankton
456 bloom magnitude on a pelagic microbial food web, *Mar Ecol Prog Ser*, 144, 211-221,
457 10.3354/meps144211, 1996.

458 Cadée, G. C., and Hegeman, J.: Phytoplankton in the Marsdiep at the end of the 20th century;
459 30 years monitoring biomass, primary production, and *Phaeocystis* blooms, *J Sea Res*, 48, 97-
460 110, 10.1016/S1385-1101(02)00161-2, 2002.

461 Campbell, B. J., Li, C., Sessions, A. L., and Valentine, D. L.: Hydrogen isotopic fractionation
462 in lipid biosynthesis by H₂-consuming *Desulfobacterium autotrophicum*, *Geochim Cosmochim*
463 *Ac*, 73, 2744-2757, 10.1016/j.gca.2009.02.034, 2009.

464 Caporaso, J. G., Kuczynski, J., Stombaugh, J., Bittinger, K., Bushman, F. D., Costello, E. K.,
465 Fierer, N., Pena, A. G., Goodrich, J. K., Gordon, J. I., Huttley, G. A., Kelley, S. T., Knights, D.,
466 Koenig, J. E., Ley, R. E., Lozupone, C. A., McDonald, D., Muegge, B. D., Pirrung, M., Reeder,
467 J., Sevinsky, J. R., Turnbaugh, P. J., Walters, W. A., Widmann, J., Yatsunencko, T., Zaneveld,
468 J., and Knight, R.: QIIME allows analysis of high-throughput community sequencing data, *Nat*
469 *Methods*, 7, 335-336, 10.1038/nmeth.f.303, 2010.



- 470 Chikaraishi, Y., Suzuki, Y., and Naraoka, H.: Hydrogen isotopic fractionations during
471 desaturation and elongation associated with polyunsaturated fatty acid biosynthesis in marine
472 macroalgae, *Phytochemistry*, 65, 2293-2300, 10.1016/j.phytochem.2004.06.030, 2004.
- 473 Chivall, D., M'Boule, D., Sinke-Schoen, D., Sinninghe Damsté, J. S., Schouten, S., and van der
474 Meer, M. T. J.: The effects of growth phase and salinity on the hydrogen isotopic composition
475 of alkenones produced by coastal haptophyte algae, *Geochim Cosmochim Acta*, 140, 381-390,
476 10.1016/j.gca.2014.05.043, 2014.
- 477 Craig, H., and Gordon, L. I.: Deuterium and oxygen 18 variations in the ocean and the marine
478 atmosphere, in: *Stable Isotopes in Oceanographic Studies and Paleotemperatures*, edited by:
479 Tongiogi, E., Consiglio Nazionale Delle Ricerche, Laboratorio Di Geologia Nucleare, Pisa, 9-
480 130, 1965.
- 481 DeSantis, T. Z., Hugenholtz, P., Larsen, N., Rojas, M., Brodie, E. L., Keller, K., Huber, T.,
482 Dalevi, D., Hu, P., and Andersen, G. L.: Greengenes, a chimera-checked 16S rRNA gene
483 database and workbench compatible with ARB, *Appl Environ Microbiol*, 72, 5069-5072,
484 10.1128/aem.03006-05, 2006.
- 485 Dirghangi, S. S., and Pagani, M.: Hydrogen isotope fractionation during lipid biosynthesis by
486 *Tetrahymena thermophila*, *Org Geochem*, 64, 105-111, 10.1016/j.orggeochem.2013.09.007,
487 2013.
- 488 Edgar, R. C.: Search and clustering orders of magnitude faster than BLAST, *Bioinformatics*,
489 26, 2460-2461, 10.1093/bioinformatics/btq461, 2010.
- 490 Fang, J., Li, C., Zhang, L., Davis, T., Kato, C., and Bartlett, D. H.: Hydrogen isotope
491 fractionation in lipid biosynthesis by the piezophilic bacterium *Moritella japonica* DSK1, *Chem*
492 *Geol*, 367, 34-38, 10.1016/j.chemgeo.2013.12.018, 2014.



- 493 Hamm, C. E., and Rousseau, V.: Composition, assimilation and degradation of *Phaeocystis*
494 *globosa*-derived fatty acids in the North Sea, *J Sea Res*, 50, 271-283, 10.1016/s1385-
495 1101(03)00044-3, 2003.
- 496 Heinzemann, S. M., Bale, N. J., Hopmans, E. C., Sinninghe Damsté, J. S., Schouten, S., and
497 van der Meer, M. T. J.: Critical assessment of glyco- and phospholipid separation by using silica
498 chromatography, *Appl Environ Microbiol*, 80, 360-365, 10.1128/aem.02817-13, 2014.
- 499 Heinzemann, S. M., Chivall, D., M'Boule, D., Sinke-Schoen, D., Villanueva, L., Damsté, J. S.
500 S., Schouten, S., and van der Meer, M. T. J.: Comparison of the effect of salinity on the D/H
501 ratio of fatty acids of heterotrophic and photoautotrophic microorganisms, *FEMS Microbiol*
502 *Lett*, 362, 10.1093/femsle/fnv065, 2015a.
- 503 Heinzemann, S. M., Villanueva, L., Sinke-Schoen, D., Sinninghe Damsté, J. S., Schouten, S.,
504 and van der Meer, M. T. J.: Impact of metabolism and growth phase on the hydrogen isotopic
505 composition of microbial fatty acids, *Front Microbiol*, 6, 1-11, 10.3389/fmicb.2015.00408,
506 2015b.
- 507 Jones, A. A., Sessions, A. L., Campbell, B. J., Li, C., and Valentine, D. L.: D/H ratios of fatty
508 acids from marine particulate organic matter in the California Borderland Basins, *Org*
509 *Geochem*, 39, 485-500, 10.1016/j.orggeochem.2007.11.001, 2008.
- 510 Klindworth, A., Pruesse, E., Schweer, T., Peplies, J., Quast, C., Horn, M., and Glöckner, F. O.:
511 Evaluation of general 16S ribosomal RNA gene PCR primers for classical and next-generation
512 sequencing-based diversity studies, *Nucleic Acids Res*, 10.1093/nar/gks808, 2012.
- 513 Li, C., Sessions, A. L., Kinnaman, F. S., and Valentine, D. L.: Hydrogen-isotopic variability in
514 lipids from Santa Barbara Basin sediments, *Geochim Cosmochim Ac*, 73, 4803-4823,
515 10.1016/j.gca.2009.05.056, 2009.
- 516 Ludwig, W., Strunk, O., Westram, R., Richter, L., Meier, H., Yadhukumar, Buchner, A., Lai,
517 T., Steppi, S., Jobb, G., Förster, W., Brettske, I., Gerber, S., Ginhart, A. W., Gross, O.,



518 Grumann, S., Hermann, S., Jost, R., König, A., Liss, T., Lüßmann, R., May, M., Nonhoff, B.,
519 Reichel, B., Strehlow, R., Stamatakis, A., Stuckmann, N., Vilbig, A., Lenke, M., Ludwig, T.,
520 Bode, A., and Schleifer, K. H.: ARB: a software environment for sequence data, *Nucleic Acids*
521 *Res.*, 32, 1363-1371, 10.1093/nar/gkh293, 2004.

522 McDonald, D., Price, M. N., Goodrich, J., Nawrocki, E. P., DeSantis, T. Z., Probst, A.,
523 Andersen, G. L., Knight, R., and Hugenholtz, P.: An improved Greengenes taxonomy with
524 explicit ranks for ecological and evolutionary analyses of bacteria and archaea, *ISMEJ*, 6, 610-
525 618, 10.1038/ismej.2011.139, 2012.

526 Mook, W.: Estuaries and the sea, in: Rozanski, K., Froehlich, K., Mook, W.G. (Eds.), Volume
527 III: Surface Water, UNESCO, Paris, 49-56, 2001.

528 Nichols, P. D., Guckert, J. B., and White, D. C.: Determination of monosaturated fatty acid
529 double-bond position and geometry for microbial monocultures and complex consortia by
530 capillary GC-MS of their dimethyl disulphide adducts, *J Microbiol Meth.*, 5, 49-55,
531 10.1016/0167-7012(86)90023-0, 1986.

532 Nichols, P. D., Skerratt, J. H., Davidson, A., Burton, H., and McMeekin, T. A.: Lipids of
533 cultured *Phaeocystis pouchetii*: Signatures for food-web, biogeochemical and environmental
534 studies in Antarctica and the Southern ocean, *Phytochemistry*, 30, 3209-3214, 10.1016/0031-
535 9422(91)83177-M, 1991.

536 Osburn, M. R., Sessions, A. L., Pepe-Ranne, C., and Spear, J. R.: Hydrogen-isotopic
537 variability in fatty acids from Yellowstone National Park hot spring microbial communities,
538 *Geochim Cosmochim Ac.*, 75, 4830-4845, 10.1016/j.gca.2011.05.038, 2011.

539 Philippart, C., van Iperen, J., Cadée, G., and Zuur, A.: Long-term field observations on
540 seasonality in chlorophyll-a concentrations in a shallow coastal marine ecosystem, the Wadden
541 Sea, *Estuaries and Coasts*, 33, 286-294, 10.1007/s12237-009-9236-y, 2010.



- 542 Philippart, C. J. M., Cadee, G. C., van Raaphorst, W., and Riegman, R.: Long-term
543 phytoplankton-nutrient interactions in a shallow coastal sea: Algal community structure,
544 nutrient budgets, and denitrification potential, *Limnol Oceanogr*, 45, 131-144, 2000.
- 545 Pitcher, A., Wuchter, C., Siedenberg, K., Schouten, S., and Sinninghe Damsté, J. S.:
546 Crenarchaeol tracks winter blooms of ammonia-oxidizing Thaumarchaeota in the coastal North
547 Sea, *Limnol Oceanogr*, 56, 2308-2318, 10.4319/lo.2011.56.6.2308, 2011.
- 548 Quast, C., Pruesse, E., Yilmaz, P., Gerken, J., Schweer, T., Yarza, P., Peplies, J., and Glöckner,
549 F. O.: The SILVA ribosomal RNA gene database project: improved data processing and web-
550 based tools, *Nucleic Acids Res*, 10.1093/nar/gks1219, 2012.
- 551 Robins, R. J., Billault, I., Duan, J.-R., Guiet, S., Pionnier, S., and Zhang, B.-L.: Measurement
552 of ^2H distribution in natural products by quantitative ^2H NMR: An approach to understanding
553 metabolism and enzyme mechanism, *Phytochem Rev*, 2, 87-102,
554 10.1023/B:PHYT.0000004301.52646.a8, 2003.
- 555 Rütters, H., Sass, H., Cypionka, H., and Rullkotter, J.: Phospholipid analysis as a tool to study
556 complex microbial communities in marine sediments, *J Microbiol Meth*, 48, 149-160,
557 10.1016/s0167-7012(01)00319-0, 2002.
- 558 Saito, K., Kawaguchi, A., Okuda, S., Seyama, Y., and Yamakawa, T.: Incorporation of
559 hydrogen atoms from deuterated water and stereospecifically deuterium labeled nicotinamide
560 nucleotides into fatty acids with the *Escherichia coli* fatty acid synthetase system, *Biochim*
561 *Biophys Acta*, 618, 202-213, 1980.
- 562 Schloss, P. D., Westcott, S. L., Ryabin, T., Hall, J. R., Hartmann, M., Hollister, E. B.,
563 Lesniewski, R. A., Oakley, B. B., Parks, D. H., Robinson, C. J., Sahl, J. W., Stres, B.,
564 Thallinger, G. G., Van Horn, D. J., and Weber, C. F.: Introducing mothur: Open-source,
565 platform-independent, community-supported software for describing and comparing microbial
566 communities, *Appl Environ Microbiol*, 75, 7537-7541, 10.1128/aem.01541-09, 2009.



- 567 Schmidt, H.-L., Werner, R. A., and Eisenreich, W.: Systematics of ^2H patterns in natural
568 compounds and its importance for the elucidation of biosynthetic pathways, *Phytochem Rev*, 2,
569 61-85, 10.1023/B:PHYT.0000004185.92648.ae, 2003.
- 570 Sessions, A. L., Jahnke, L. L., Schimmelfmann, A., and Hayes, J. M.: Hydrogen isotope
571 fractionation in lipids of the methane-oxidizing bacterium *Methylococcus capsulatus*, *Geochim*
572 *Cosmochim Ac*, 66, 3955-3969, 10.1016/s0016-7037(02)00981-x, 2002.
- 573 Sintes, E., Witte, H., Stoderegger, K., Steiner, P., and Herndl, G. J.: Temporal dynamics in the
574 free-living bacterial community composition in the coastal North Sea, *FEMS Microbiol Ecol*,
575 83, 413-424, 10.1111/1574-6941.12003, 2013.
- 576 Sørensen, N., Daugbjerg, N., and Richardson, K.: Choice of pores size can introduce artefacts
577 when filtering picoeukaryotes for molecular biodiversity studies, *Microb Ecol*, 65, 964-968,
578 10.1007/s00248-012-0174-z, 2013.
- 579 Vaezi, R., Napier, J. A., and Sayanova, O.: Identification and functional characterization of
580 genes encoding omega-3 polyunsaturated fatty acid biosynthetic activities from unicellular
581 microalgae, *Marine Drugs*, 11, 5116-5129, 10.3390/md11125116, 2013.
- 582 Valentine, D. L., Sessions, A. L., Tyler, S. C., and Chidthaisong, A.: Hydrogen isotope
583 fractionation during H_2/CO_2 acetogenesis: hydrogen utilization efficiency and the origin of
584 lipid-bound hydrogen, *Geobiology*, 2, 179-188, 10.1111/j.1472-4677.2004.00030.x, 2004.
- 585 Werner, J. J., Koren, O., Hugenholtz, P., DeSantis, T. Z., Walters, W. A., Caporaso, J. G.,
586 Angenent, L. T., Knight, R., and Ley, R. E.: Impact of training sets on classification of high-
587 throughput bacterial 16s rRNA gene surveys, *ISMEJ*, 6, 94-103, 10.1038/ismej.2011.82, 2012.
- 588 Zhang, X. N., Gillespie, A. L., and Sessions, A. L.: Large D/H variations in bacterial lipids
589 reflect central metabolic pathways, *Proc Natl Acad Sci USA*, 106, 12580-12586,
590 10.1073/pnas.0903030106, 2009a.



591 Zhang, Z., and Sachs, J. P.: Hydrogen isotope fractionation in freshwater algae: I. Variations
592 among lipids and species, *Org Geochem*, 38, 582-608, 10.1016/j.orggeochem.2006.12.004,
593 2007.

594 Zhang, Z., Sachs, J. P., and Marchetti, A.: Hydrogen isotope fractionation in freshwater and
595 marine algae: II. Temperature and nitrogen limited growth rate effects, *Org Geochem*, 40, 428-
596 439, 10.1016/j.orggeochem.2008.11.002, 2009b.

597

598 **Figure and tables legends**

599 **Figure 1**

600 $\epsilon_{\text{average}}$ values compared to chlorophyll *a* concentrations. $\epsilon_{\text{fattyacids}}$ is the weighted average of
601 *n*C14:0, *n*C16:1, *n*C16:0, *n*C18:0 fatty acids and the *n*C20:5 PUFA from Jetty samples taken
602 from August 2010 – December 2011.

603 **Figure 2**

604 Phytoplankton diversity and abundance (measured in cells L⁻¹) observed in the coastal North
605 Sea between August 2010 – December 2011.

606 **Figure 3**

607 Order-level bacterial diversity and abundance in North Sea water based on the 16S rRNA gene
608 sequence.

609 **Figure 4**

610 Relative abundance of fatty acids and chlorophyll *a* concentration in North Sea SPM. (a)
611 *n*C14:0, (b) *n*C16:1, (c) *n*C16:0, (d) *n*C18:x, (e) *n*C18:0, (f) *n*C20:5 PUFA and chlorophyll *a*.

612 **Figure 5**



613 The D/H fractionation between fatty acids and North Sea water for fatty acids derived from
614 suspended particulate matter in North Sea water samples. Plotted are the the $\epsilon_{\text{lipid/water}}$ values of
615 $nC_{14:0}$, $nC_{16:1}$, $nC_{16:0}$, $nC_{18:0}$ fatty acids and $nC_{20:5}$ PUFA. Error bars are the standard
616 deviation of the duplicate measurements of the fatty acids.

617 **Table 1**

618 D/H fractionation between fatty acids and North Sea water for fatty acids derived from
619 suspended particulate matter in North Sea water samples.

620

621

622



Table 1

Date	Salinity	δD_{water} [‰] (estimated)	$\epsilon_{\text{lipid/water}}$ [‰]					$\epsilon_{\Sigma\text{FA}}$ [‰] weighted average C14, C16:1, C16, C18
			C14:0	C16:1	C16:0	C18:0	C20:5 PUFA	
16/08/10	27.3	-8.2	-212±0	-194±1	-194±2	-178±3	-185±1	-196
30/08/10	29.7	-4.1	-218±2	-198±2	-186±1	-182±0	-195±1	-197
15/09/10	30	-3.6	-213±2	-203±1	-194±0	-183±1	-177±1	-201
28/09/10	24.7	-12.6	-209±0	-188±0	-182±1	-187±1	-197±2	-190
15/11/10	30	-3.6	-211±2	-200±0	-179±1	-197±0	N.D.	-192
26/11/10	24.8	-12.4	-216±2	-192±1	-178±2	-193±2	N.D.	-191
10/12/10	27.1	-8.5	-218±0	-181±0	-184±0	-195±0	N.D.	-191
17/12/10	24.1	-13.6	-221±2	-182±1	-183±1	-177±2	N.D.	-188
10/01/11	27.8	-7.3	-215±3	-195±1	-180±0	-198±0	N.D.	-191
24/01/11	23.0	-15.5	-200±2	-179±0	-183±0	-180±1	-197±2	-183
17/02/11	29.3	-4.8	-219±1	-204±0	-191±0	-203±1	N.D.	-200
08/03/11	25.8	-10.7	-218±6	-206±2	-197±1	-173±4	-227±8	-203
23/03/11	26.8	-9.0	-234±1	-209±1	-198±0	-182±5	-234±1	-208
05/04/11	29.2	-4.9	-219±0	-206±3	-205±1	-208±5	-220±3	-208
19/04/11	27.7	-7.5	-229±0	-219±1	-215±0	N.D.	-235	-214
03/05/11	31.1	-1.7	-237±5	-224±1	-213±2	-210±2	-235±2	-223
18/05/11	31.8	-0.5	-219±0	-205±0	-197±2	-177±0	-213±1	-203
17/06/11	32.0	0.7	-225±2	-211±0	-196±3	-191±0	N.D.	-206
30/06/11	31.2	-1.6	-224±1	-208±1	-200±1	-173±6	-212	-209
15/07/11	30.0	-3.6	-202±1	-192±0	-185±0	-178±2	-215±2	-191
27/07/11	26.3	-9.9	-213±3	-192±3	-195±0	-172±0	-193±6	-194
08/08/11	29.4	-4.6	-219±6	-198±2	-197±3	-176±7	-231±2	-200
22/08/11	26.9	-8.9	-224±1	-195±0	-182±4	-183±2	-195	-196
06/09/11	26.8	-9.0	-217±5	-210±0	-213±3	-209±1	-211±1	-212
21/09/11	30.1	-3.4	-215±0	-201±0	-182±0	-191±1	N.D.	-193
11/10/11	32.8	1.2	-214±3	-192±0	-184±2	-189±3	-227	-192
28/10/11	32.2	0.1	-217±0	-188±0	-181±2	-184±1	-207±4	-189
15/11/11	28.9	-5.5	-208±12	-194±2	-187±4	-179±6	-217	-192
28/11/11	31.7	-0.7	-217±0	-192±0	-189±1	-180±2	-197±1	-195
16/12/11	31.7	-0.7	-198±6	-179±2	-173±3	-187±2	N.D.	-180

nC16:1*: double bond at the ω 7 position

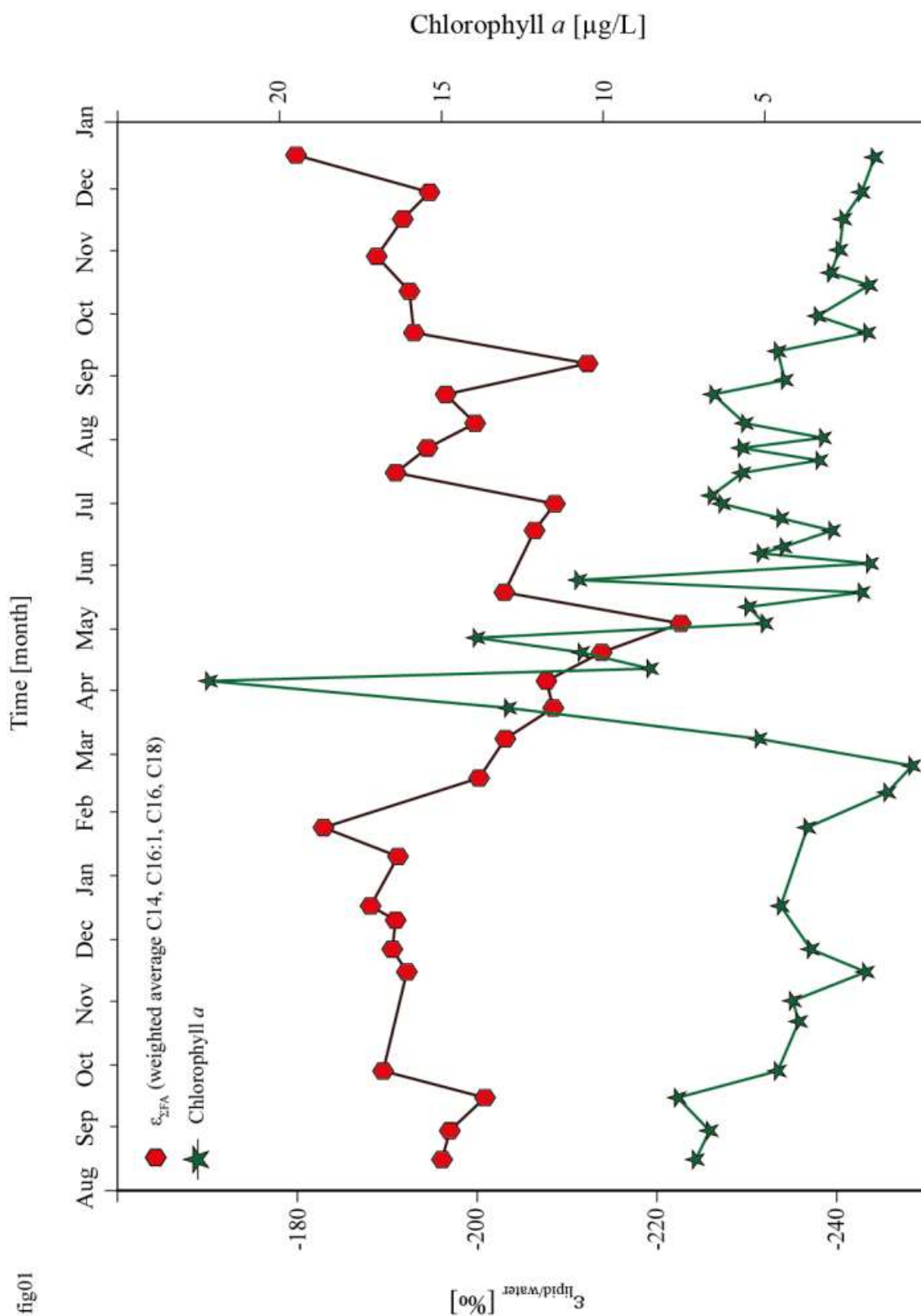


fig01

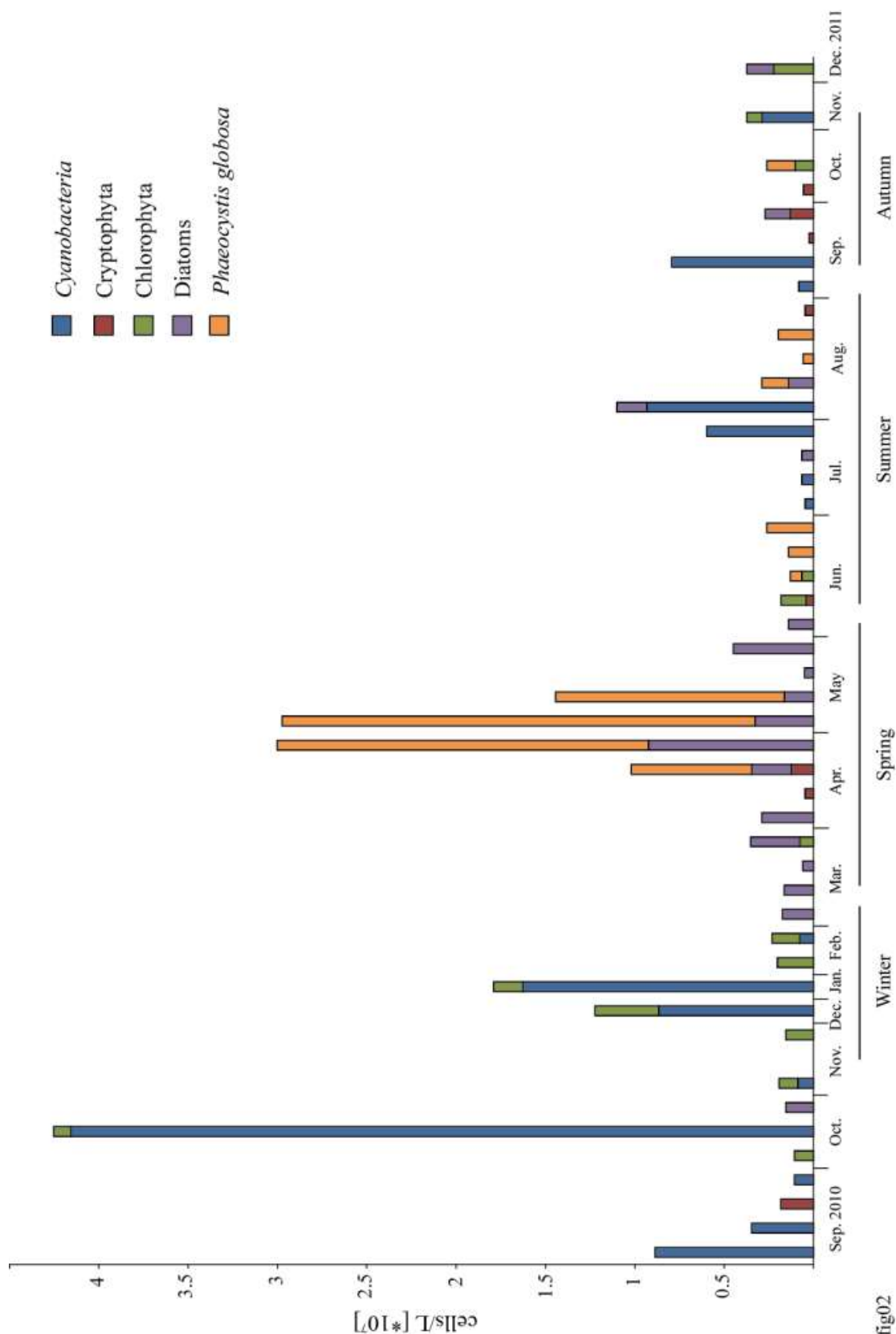


fig02 30

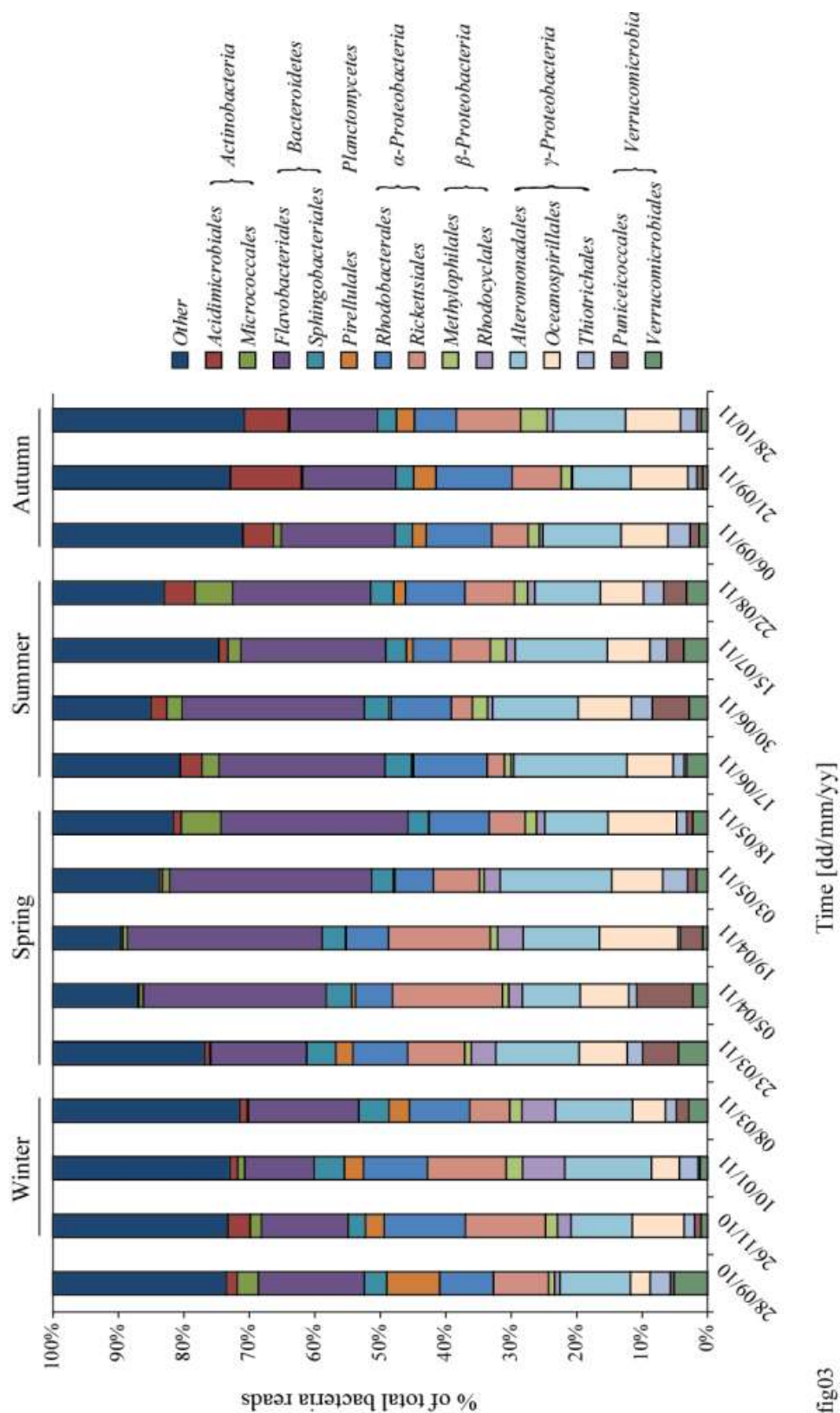


fig03

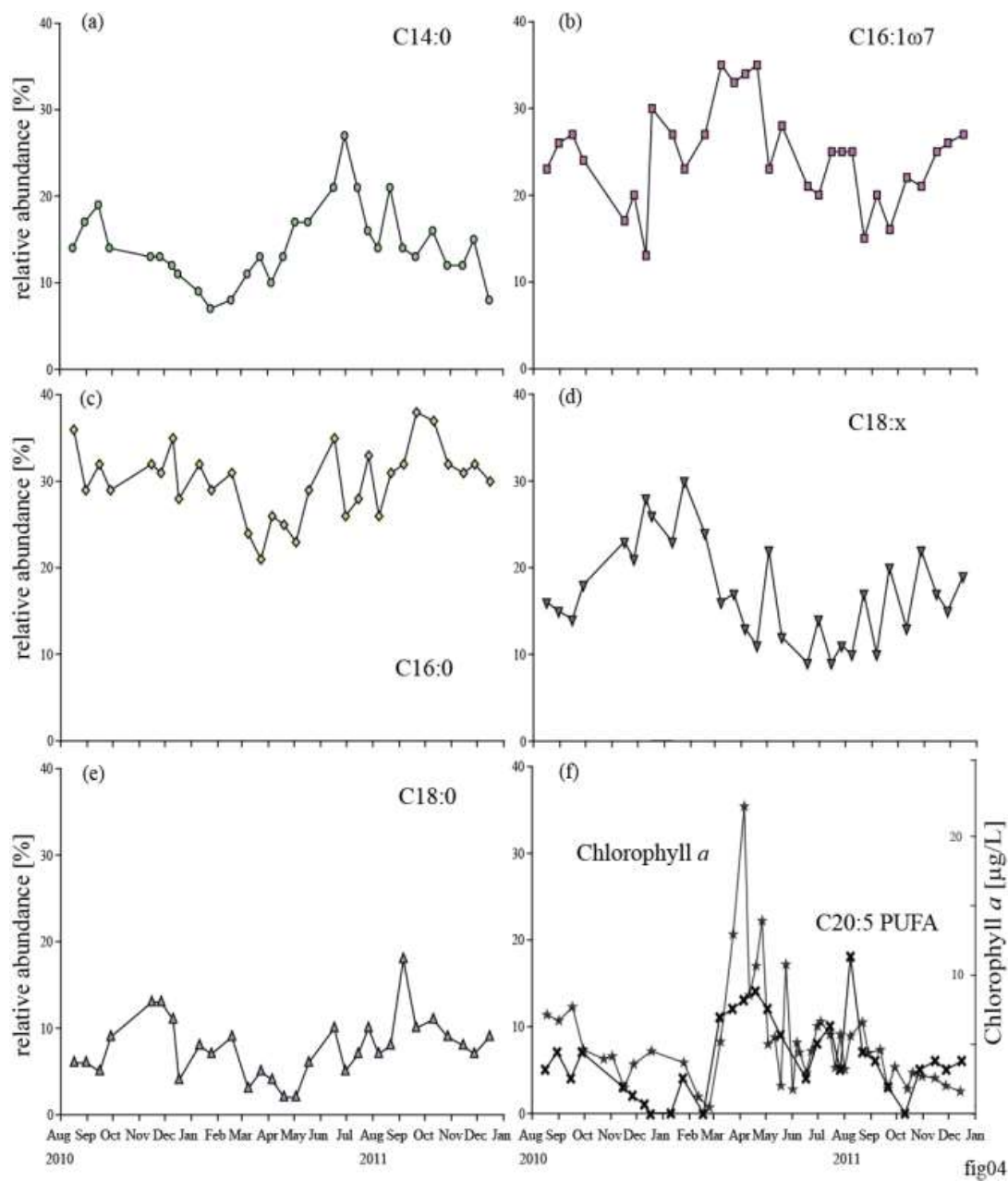


fig04

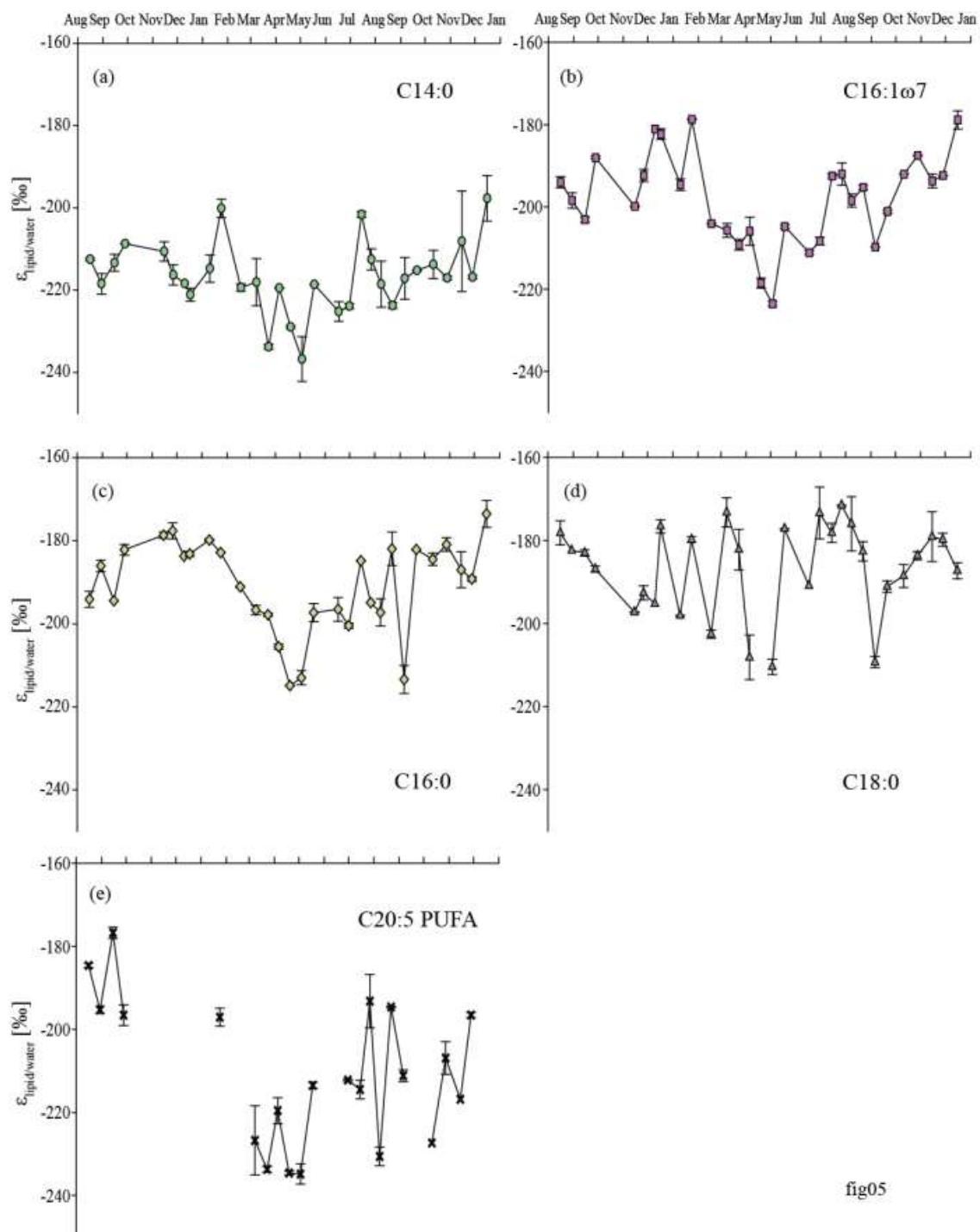


fig05